***How to Cite**:* Zhinzhilo, V.A., Litvinova, A.Yu., Lyamina, V.M., Dzhardimalieva, G.I., & Uflyand, I.E. (2022) Coordinating Polymers Based on Nickel(II) and Cobalt(II) Trimesinates as Promising Adsorbents of Organic Dyes. *Bulletin of the University of Karaganda – Chemistry, 107(3), 239-253.* https://doi.org/10.31489/2022Ch3/3-22-20

Article Received: 31 May 2022 | Revised: 28 June 2022 | Accepted: 14 July 2022 | Published online: 26 July 2022

UDC 544.7+544.023.57 https://doi.org/10.31489/2022Ch3/3-22-20

V.A. Zhinzhilo[1], A.Yu. Litvinova[1], V.M. Lyamina[1], G.I. Dzhardimalieva[2, 3*], I.E. Uflyand[1]

[1]*Southern Federal University, Rostov-on-Don, Russian Federation;*
[2]*Institute of Problems of Chemical Physics RAS, Chernogolovka, Russian Federation;*
[3]*Moscow Aviation Institute (National Research University), Moscow, Russian Federation*
*(*Corresponding author's e-mail: dzhardim@icp.ac.ru)*

Coordinating Polymers Based on Nickel(II) and Cobalt(II) Trimesinates as Promising Adsorbents of Organic Dyes

Metal-organic frameworks (MOFs) are crystalline compounds consisting of metal ions coordinated by bridging organic ligands. Depending on the coordination geometry of the metal and the direction of the bond of donor atoms, as well as on the geometry of the bridging ligand, 1D, 2D, or 3D polymer structures are formed. The characteristic features of metal-organic frameworks are low density, high porosity and crystallinity, and large specific surface. Wide attention is paid to the technological aspects of creating such materials and their integration into various devices. To obtain MOFs, various synthetic approaches have been developed based on precipitation reactions at room temperature and under convective heating, including hydrothermal and solvothermal syntheses. In this work, metal organic framework structures based on nickel and cobalt trimesinates were synthesized by a modified procedure by reacting nickel acetate and cobalt nitrate with trimesic acid in the presence of alkali. The obtained compounds were used to study the adsorption of Congo Red and Methylene blue organic dyes from their aqueous solutions. The degree of adsorption depends on temperature and reaches a value of 97% for Congo Red, while for Methylene blue it is 83%. The mechanisms and characteristic parameters of the adsorption process were analyzed using empirical models of Langmuir, Temkin, and Freundlich isotherms, of which the adsorption process was optimally described by the Freundlich model. The calculated thermodynamic parameters indicate the spontaneity of the process and its insignificant endothermic character.

Keywords: metal organic framework structures, coordination polymers, trimesic acid, pollutants, adsorption, Congo Red, methylene blue, thermodynamic parameters, adsorption isotherms, adsorption capacity.

Introduction

Metal–organic framework structures (MOFs) play an important role in science and technology since they are widely used in catalysis [1], separation and selective purification of substances [2], are necessary for the creation of nonlinear optical materials [3], and the synthesis of new compounds capable of a magnetic phase transition at high temperatures [4]. Due to the wide variety of organic and inorganic building blocks that make up MOFs, there are a huge number of opportunities for designing such materials with defined structures and desired properties [5]. In recent years, there has been a noticeable interest in MOFs based on benzenepolycarboxylic acids. Such MOFs are characterized by a regular structure and constant porosity after thermal/vacuum activation, which allows them to encapsulate various guest molecules in a bulk structure and makes them promising solid materials for a number of applications such as gas storage and separation of substances in solutions. In addition, they attract the attention of researchers because of their different modes of coordination with respect to metal ions, in particular, exhibiting monodentate, bridging, chelating modes, etc. For example, C3v-symmetrical trimesic (1,3,5-benzenetricarboxylic) acid has been used to create MOF systems with interesting application possibilities. The first representative of this series of MOFs was synthesized in 1999 [6] and designated as HKUST-1 (HKUST – Hong Kong University of Science and Technology). A distinctive feature of Cu(II)-containing MOFs is the presence of binuclear fragments of the "Chinese lantern" type. This structure serves as a benchmark both in terms of stability and the ability to absorb various sorbates. Importantly, HKUST-1 stands out as a representative example, forming an isostructural series with other transition metal ions, including Zn [7], Mo [8], Cr [9, 10], Fe [11], Ni [12], Ru [13, 14], Co [15]. These MOFs have two important features: (1) the metal Lewis acid sites available for coordination by donor substrates are located within the pore walls; (2) materials can be activated (including removal of axially coordinated molecules) without destroying the underlying scaffold. An important role in their properties is played by a variety of supramolecular structures and such structural details as pores, channels, and voids of nanome-

ter dimensions. The latter circumstance makes it possible to use such polybenzene carboxylates as selective adsorbents, catalysts, electrodes for supercapacitors, etc. [16–21]. MOFs are of considerable interest for the extraction of technogenic pollutants, in particular, organic dyes from wastewater and the return of the latter to nature without damaging it [22]. It is important that many coordination polymers, in turn, are biologically and environmentally safe compounds. All metals and linkers can be used even for biomedical applications, but at different doses depending on several parameters, such as degradation kinetics, biodistribution, accumulation in tissues and organs, etc.

The synthesis of MOFs is usually carried out by the solvo- or hydrothermal method [23]. At present, the strategies for the synthesis of MOFs are well-developed, and, particularly, they are described in the literature for nickel and cobalt trimesinates [24, 25]. However, such methods are often laborious and require special equipment and a long time; at the same time, as shown in [26], they can be successfully replaced by more accessible synthetic methods carried out by the "RT" method.

The aim of this work is to develop procedures for the synthesis of nickel(II) and cobalt(II) complexes based on trimesic acid in aqueous solutions without the use of modulating agents. In addition, the investigation task is to study the ability of the resulting nickel and cobalt trimesinates to adsorb organic dyes from their aqueous solutions.

Experimental

Materials

Commercially available reagents were used in the work, namely trimesic acid (98 %, Acros Organics, cat. no. 105350500), NaOH (technical, AO Kaustik), $Ni(CH_3COO)_2{\cdot}4H_2O$ (99 %+, Acros Organics, cat. no. 223141000), $Co(NO_3)_2{\cdot}6H_2O$ (99 %, Acros Organics, cat. no. 213091000). Ethanol, methanol, ethyl acetate, chloroform, and diethyl ether were used as solvents (all of the above reagents were produced by JSC Reakhim, chemically pure). All reagents were not subjected to additional preparation and purification. The solvents were dried by standard procedures. The sorbates were cationic Methylene blue and anionic Congo Red (Sigma-Aldrich, cat. nos. 556416 and B24310.14).

The synthesis of nickel and cobalt trimesinates consisted of two stages. In the first stage, a soluble form of trimesic acid was obtained in the form of a sodium salt. To an aqueous solution containing 0.09 mol of sodium hydroxide (in 50 mL of water), 0.03 mol of acid was added while heating to 80 °C, the process was controlled by the pH value of the solution, carrying it out in the range of 5.5–6.0. In the second stage, an aqueous solution containing 0.09 mol of $Ni(CH_3COO)_2{\cdot}4H_2O$ or $Co(NO_3)_2{\cdot}6H_2O$ (calculated as anhydrous salt) in 30 mL of hot water was introduced into the resulting sodium (I) trimesinate solution. The resulting mixture was stirred for 6 h, maintaining the temperature at 80°C, and left for crystallization for 12 h at room temperature. Cobalt(II) trimesinate precipitates almost immediately as a pink fine crystalline precipitate (hydrated form), while nickel(II) trimesinate precipitates within a few hours as a light green crystalline precipitate (hydrated form). The precipitated crystals were separated by filtration on a glass filter, washed with hot water and then with alcohol, and dried in air to an air-dry state. The dried product was treated sequentially in absolute ethanol, dry ethyl acetate, and chloroform, keeping in each solvent with constant stirring on a magnetic stirrer for 12 h. In the final stage, the compound was dried in air and kept for 36 h in a dynamic vacuum at a temperature of 150 °C (nickel(II) trimesinate) and 180 °C (cobalt(II) trimesinate). As a result, anhydrous salts were obtained with a yield of 73% (nickel(II) trimesinate), which is a yellow-green loose powder, and 88 % (cobalt(II) trimesinate) in the form of loose violet crystals. The weight loss on drying was 25.92 % for nickel(II) trimesinate (theoretical calculation for a loss of 12 water molecules, 26.6 %), for cobalt(II) trimesinate, 26.1 % (theoretical calculation for the loss of 12 water molecules is 26.57 %), which is in good agreement with the literature data. The resulting compounds were characterized by elemental analysis, the results are presented in Table 1.

Elemental analysis was performed on a Vario Micro cube analyzer (Elementar GmbH, Langenselbold). Ni and Co were determined on an AAS-3 atomic absorption spectrometer (Zeiss, Jena). X-ray phase analysis was performed on a Phywe XR 4.0 instrument (CuKα, λ = 0.15418 nm, scanning speed 2 deg/min, step size 0.02°). Fourier transform infrared spectra were obtained on a Perkin-Elmer Spectrum 100 FTIR spectrometer using KBr pellets and Softspectra data analysis software (Shelton, CT). Scanning electron microscopy was performed on a ZEISS Crossbeam 340 instrument with an accelerating voltage of 3 kV. Secondary electrons were detected using an Everhart-Thornley detector (SE2) with a change in magnification from 1.92 to

50000 times. The dye concentration was determined using a UV-visible spectrophotometer (Varian, Cary 50) at λ_{max} = 492 nm (Congo Red) and 664 nm (Methylene blue), respectively [28].

Table 1

Elemental Analysis of Synthesized nickel(II) and cobalt(II) trimesinates

Hydrated form				
Element	Found, %	Calculated for $C_{18}H_6O_{12}Ni_3 \cdot 12H_2O$, %	Found, %	Calculated for $C_{18}H_6O_{12}Co_3 \cdot 12H_2O$, %
C	25.93	26.58	26.93	26.56
H	3.44	3.70	3.58	3.69
Ni	22.12	21.67	–	–
Co	–	–	22.4	21.74
Anhydrous form				
Element	Found, %	Calculated for $C_{18}H_6O_{12}Ni_3$, %	Found, %	Calculated for $C_{18}H_6O_{12}Co_3$, %
C	35.3	36.2	36.8	36.17
H	1.1	1.00	0.99	1.00
Ni	30.0	29.5	–	–
Co	–	–	30.2	29.6

For adsorption studies, the dye solution with a volume of 200 mL and an initial concentration of C_0 = 20 mg/L was placed in a beaker with a capacity of 300 mL, thermostated at 283, 293, and 308 K on a magnetic stirrer, adjusting the rotation speed so that mixing was effective, but air in the liquid phase was not drawn in. When the desired temperature was reached, an adsorbent was introduced, which was the synthesized MOF. To determine the maximum adsorption capacity, a series of experiments was carried out, in which adsorbents were introduced into the dye solution under the same conditions, equal to 6.25, 12.5, 25, 50, 100 mg, and stirring was continued for 3 h, considering that this time was sufficient until equilibrium was reached in system. After the specified time, the mixture was centrifuged, and the residual concentration of the dye was determined in the supernatant.

The adsorption capacity of the MOF in aqueous solutions of Methylene blue and Congo Red at 283, 293, and 308 K was determined by suspending 0.1 g of MOF in 200 mL of the initial dye solution (C_0 = 20 mg/L) and the mixture was stirred. At predetermined time intervals, 10 mL of the mixture was taken, quickly centrifuged, and the residual concentration of the dye in the solution was determined. The obtained results were compared with the calibration curve and the equivalent concentration of the dye in a given time period was determined.

To obtain adsorption isotherms, 20 mL of a dye solution of various concentrations (10–200 mg/L) was added to a sample of the adsorbent (10 mg) and stirred for 3 hours. This time was considered sufficient to achieve equilibrium. Then a portion of the solution was taken and the concentration of the dye was determined.

The adsorption value was calculated using the following equations:

$$q_t = \frac{(C_0 - C_t)V}{m}; \quad (1)$$

$$q_e = \frac{(C_0 - C_e)V}{m}, \quad (2)$$

where q_t and q_e — the amounts (mg/g) of the dye adsorbed on the adsorbent at time t and in the equilibrium state, respectively; C_0, C_t, and C_e — the concentrations of the dye in the solution (mg/L) at the initial stage, at time t, and in the state of equilibrium, respectively; m (g) and V (L) — the amount of adsorbent and the volume of dye solution, respectively.

The degree of adsorption R (%) (extraction ratio of the sorbate) was calculated by the formula:

$$R(\%) = \frac{(C_0 - C_e)}{C_0} \times 100. \quad (3)$$

Results and Discussion

Nickel(II) and cobalt(II) trimesinates were synthesized by direct interaction of metal salts and trimesic acid in water in the presence of alkali. The morphology of the synthesized nickel and cobalt(II) trimesinates was studied by scanning electron microscopy. Nickel(II) trimesinate consists of prismatic crystals ranging in size from 3×1.2×0.6 (65 %) to 7.3×2.3×1 μm (20 %), some of which are visualized as broken. A characteristic feature of the crystals is their layered character (Fig. 1A). Cobalt(II) trimesinate is also formed by elongated prismatic crystals, more uniform and monolithic (with a smooth surface) compared to nickel(II) trimesinate. The size of the crystals varies from 3.1×0.6×0.6 (15 %) to 3.6×0.5×0.5 (80 %) μm, and less than 2 % is represented by wide but short crystals (in the form of tablets) with dimensions of 2.6×1.86×0.33 μm (Fig. 1B).

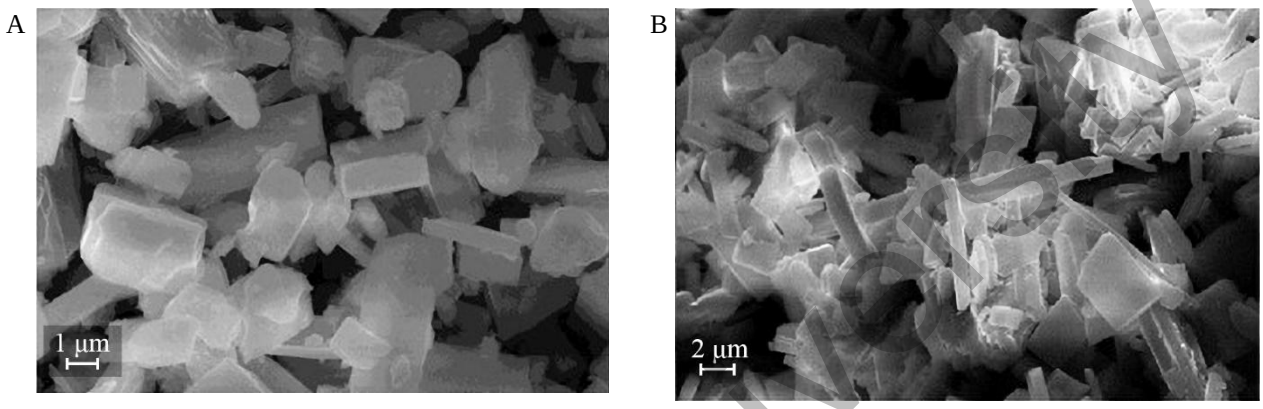

Figure 1. Images of nickel(II) (A) and cobalt(II) (B) trimesinate crystals obtained by scanning electron microscopy

X-ray phase analysis was carried out to identify the obtained compounds. The observed sharp and distinct diffraction peaks indicate that the prepared samples of nickel and cobalt trimesinates have good crystallinity and high phase purity. All positions of the diffraction peaks are in good agreement with the results of modeling performed in the program for processing X-ray phase analysis data "Match-3" (Fig. 2) and previously published works [24, 25]. In addition, X-ray diffraction data show that the peaks intensity does not completely match the theoretical calculation and may indicate the presence of crystals with a preferred growth orientation that are in the state of formation. The diffraction patterns of both compounds have much in common, which characterizes the compounds as isostructural [29].

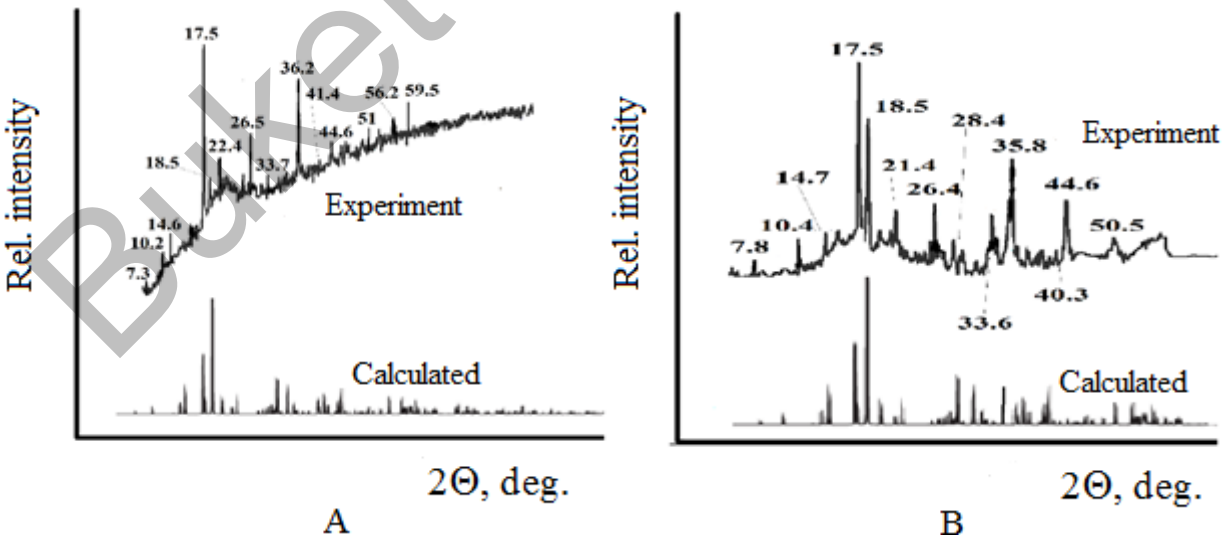

Figure 2. Calculated and experimental diffraction patterns of nickel(II) (A) and cobalt(II) (B) trimesinates

The IR spectra of trimesic acid and synthesized compounds were studied to determine the coordination mode of the organic ligand. The IR spectrum of trimesic acid shows bands with an absorption maximum in

the region of 1720, 1430 and 1276 cm^{-1}. The first band is characteristic of stretching vibrations of the carboxyl group; the other two are due to a combination of planar bending vibrations of the hydroxyl group and stretching vibrations of the C–O bond in carboxylic acid dimers. The IR spectra of nickel and cobalt trimesinates are almost identical and are in satisfactory agreement with the results previously published in the literature [25]. The IR spectrum of the resulting nickel(II) and cobalt(II) trimesinates lacks a band at 1720 cm^{-1}, which indicates complete deprotonation of carboxyl groups and their binding to metal ions. The latter is confirmed by the formation of the M–O bond and is proved by the formation of a new strong absorption band in the region of 765 cm^{-1} (Ni) and 768 cm^{-1} (Co). At the same time, absorption bands appear, which are not recorded in the spectrum of trimesic acid, located in the region of 1562 cm^{-1} (Ni) and 1565 cm^{-1} (Co), characteristic of asymmetric stretching vibrations of carboxylate ions. Stretching symmetric vibrations of this anion are fixed in the region of 1375 cm^{-1} (Ni) and 1376 cm^{-1} (Co). The difference between the wave numbers of asymmetric and symmetric stretching vibrations of carboxylate anions is 187 cm^{-1} (Ni) and 189 cm^{-1} (Co), which allows us to conclude that in this case, a bidentate-bridging mode of coordination of the carboxylate ion is possible.

The ability of nickel(II) and cobalt(II) trimesinates to adsorb organic dyes from aqueous solutions at different temperatures was studied (Fig. 3). The dependences found indicate that the adsorption value tends to slightly increase with increasing temperature in the studied temperature range.

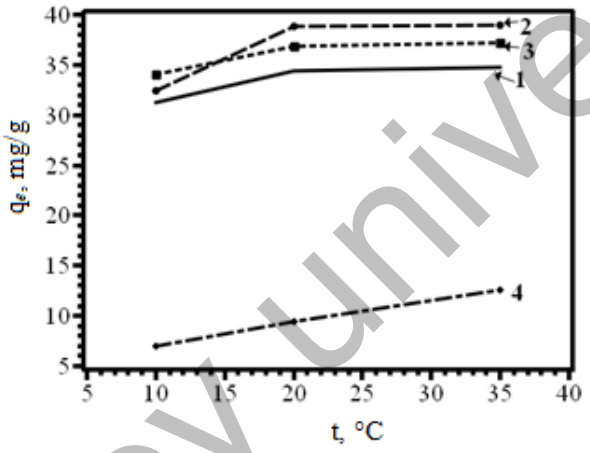

1 — Nickel(II) trimesinate – Congo Red; *2* — nickel(II) trimesinate – Methylene blue;
3 — cobalt (II) trimesinate – Congo Red; *4* — cobalt(II) trimesinate – Methylene blue

Figure 3. Effect of temperature on the adsorption of dyes in systems

The extraction efficiency versus the contact time of the sorbate with the sorbent is shown in Fig. 4. It can be seen from the presented figure that the degree of adsorption is higher in the case of Congo Red, reaching a value of 97 %, while for Methylene blue it is about 83 %.

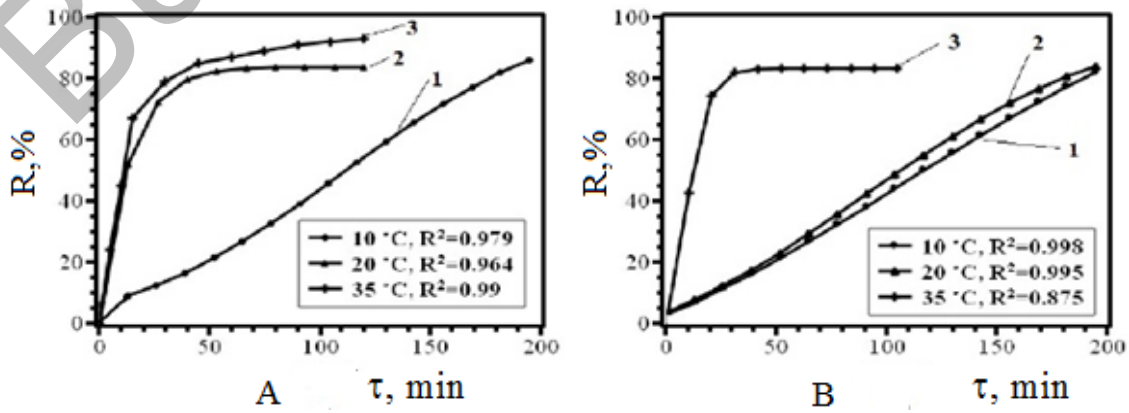

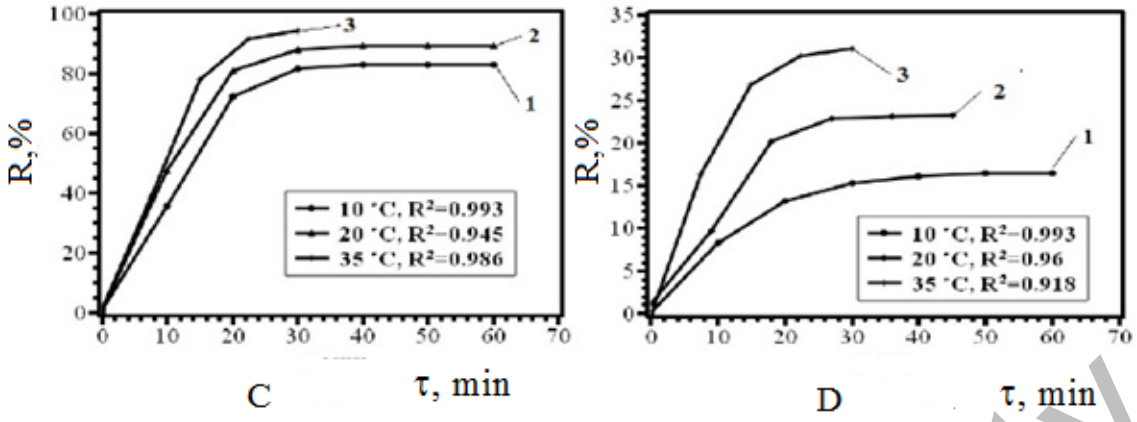

Figure 4. Time dependence of the adsorption degree of Congo Red (A, C) and Methylene blue (B, D) by nickel (A, B) and cobalt (C, D) trimesinates at different temperatures

The data obtained in the study of the adsorption of organic dyes by the studied MOFs were analyzed using various adsorption models. Preference was given to the models of Langmuir, Freundlich, and Temkin.

Langmuir adsorption model. This model gives a quite specific quantitative characteristic of the adsorption process at low and high sorbate concentrations. The Langmuir adsorption isotherm assumes that adsorption occurs at certain homogeneous sites within the adsorbent and has been successfully applied in many monolayer adsorption sorption processes [30]. The Langmuir isotherm can be written as [31]:

$$q_e = \frac{q_{max} K_L C_e}{1 + K_L C_e}, \quad (4)$$

where K_L — the Langmuir constant (L/mg) related to the set of binding sites and the free energy of adsorption; q_{max} — the limiting adsorption, which expresses the concentration of the dye during the formation of a monolayer on the adsorbent (mg/g).

Equation (4) is usually represented in a linear form:

$$\frac{C_e}{q_e} = \frac{1}{K_L q_{max}} + \frac{C_e}{q_{max}}. \quad (5)$$

For the Langmuir equation, the favorable nature of adsorption can be expressed in terms of the dimensionless equilibrium parameter R_L, which is determined as follows:

$$R_L = \frac{1}{1 + K_L C_0}. \quad (6)$$

R_L values indicate that the process type is irreversible ($R_L = 0$), favorable ($0 < R_L < 1$), linear ($R_L = 1$) or unfavorable ($R_L > 1$) [32].

Freundlich adsorption model. The empirical equation of the Freundlich isotherm is used to describe heterogeneous systems with medium coverages of the adsorbent surface [30]. It looks like this:

$$q_e = k_F C_e^{1/n_F}, \quad (7)$$

where K_F — a constant showing the adsorption capacity of the adsorbent ($mg^{1-1/n} L^{1/n} g^{-1}$); $1/n$ — an empirical constant related to the adsorption driving force.

The value of $1/n$ quantitatively determines the conditions favoring adsorption and characterizes the degree of inhomogeneity of the MOF surface [33]:

$$K_F = \frac{q_{max}}{C_0^{\frac{1}{n}}}. \quad (8)$$

It is necessary to work with a constant initial concentration C_0 and a variable mass of the adsorbent to determine the maximum adsorption (q_{max}).

Temkin's adsorption model. The Temkin model takes into account sorbent-sorbate interactions and assumes that the heat of adsorption as a function of the temperature of all molecules in the layer will decrease linearly as the layer is filled [34]. However, this model has specific limitations associated with the impossibility of using it at low or high sorbate concentrations in the solution. This model contains a parameter that takes into account interactions between adsorption sites and sorbate.

The experimental results on the determination of adsorption isotherms were processed according to the Temkin equations:

$$q_e = \frac{RT}{b} \ln K_t C_e; \quad (9)$$

$$B_t = \frac{RT}{b}. \quad (10)$$

Equation (9) can be expressed linearly:

$$q_e = B_T ln K_T + B_T ln C_e, \quad (11)$$

where T — the absolute temperature, K; R — the universal gas constant, R = 8.314 J/(mol K); K_T — the equilibrium constant; b — the constant associated with the heat of adsorption, J/mol; B_T — the Temkin isotherm constant.

The calculated values of the maximum adsorption and adsorption equilibrium constants at different temperatures are given in Table 2. The R_L values for dye adsorption on MOFs at different temperatures are less than 1 and greater than zero, which indicates the conditions favoring adsorption. In addition, experimental data show that the adsorption process is optimally described by the Freundlich model. The values of the coefficient 1/n range from 0 to 1, which also indicates favorable conditions for adsorption, while the lowest values are observed for the cobalt trimesinate – Methylene blue system, which is in good agreement with other experimental data and generally characterizes cobalt trimesinate as a relatively inefficient adsorbent with respect to cationic dyes (Methylene blue), while its adsorption capacity for anionic dyes (Congo Red) is satisfactory.

Table 2

Parameter values of adsorption isotherms

Model	Adsorbent	Sorbate	Parameter	*T*, K		
				283	293	308
1	2	3	4	5	6	7
Langmuir	Nickel(II) trimesinate	Congo Red	q_{max}	123.4	128.2	161.3
			K_L	0.81	0.6	0.62
			R_L	0.058	0.076	0.074
			R^2	0.896	0.994	0.956
		Methylene blue	q_{max}	107.5	119	153.8
			K_L	4.65	8.4	6.5
			R_L	0.01	0.006	0.007
			R^2	0.967	0.993	0.895
	Cobalt(II) trimesinate	Congo Red	q_{max}	120.5	143	161
			K_L	8,3	7.0	6.2
			R_L	0.006	0.007	0.008
			R^2	0.862	0.981	0.902
		Methylene blue	q_{max}	133	149	156
			K_L	3.75	2.23	0.45
			R_L	0.013	0.022	0.1
			R^2	0.864	0.905	0.814
Freundlich	Nickel(II) trimesinate	Congo Red	$1/n$	0.81	0.6	0.57
			K_F	0.51	0.690	0.75
			R^2	0.965	0.932	0.937
		Methylene blue	$1/n$	0.72	0.7	0.63
			K_F	0.7	2.3	4.1
			R^2	0.895	0.905	0.9
	Cobalt(II) trimesinate	Congo Red	$1/n$	0.72	0.7	0.65
			K_F	0.33	0.69	0.78
			R^2	0.911	0.932	0.92
		Methylene blue	$1/n$	0.71	0.67	0.75
			K_F	0.35	0.1	0.33
			R^2	0.83	0.815	0.865

Continuation of Table 2

1	2	3	4	5	6	7
Temkin	Nickel(II) trimesinate	Congo Red	b	36.18	40.58	46.53
			K_T	2.3	5.41	6.47
			R^2	0.929	0.944	0.958
		Methylene blue	b	33.6	38.64	44.9
			K_T	2.66	2.0	0.57
			R^2	0.926	0.949	0.968
	Cobalt(II) trimesinate	Congo Red	b	31.37	27.98	32.8
			K_T	12.5	43.5	78
			R^2	0.943	0.975	0.982
		Methylene blue	b	37.93	40.58	45.1
			K_T	2.48	0.9	0.45
			R^2	0.946	0.991	0.998

In addition, an analysis of dye adsorption isotherms shows that they refer to monomolecular adsorption isotherms and the curves monotonically approach a certain limiting value corresponding to monolayer filling.

The data obtained during the study of the adsorption process were analyzed using kinetic models of pseudo-first and pseudo-second order reactions. An equation that satisfactorily describes adsorption from a liquid medium by solid adsorbents was proposed by Lagergren and can be represented in the differential form as [35]:

$$\frac{dq_t}{dt} = k_1(q_e - q_t), \tag{12}$$

where k_1 (min^{-1}) — the adsorption rate constant of the pseudo-first order model.

After a certain integration from $t = 0$ to $t = t$ and from $q = 0$ to $q = q_e$, equation (12) takes the form:

$$\ln (q_e - q_t) = \ln q_e - k_1 t. \tag{13}$$

The differential form of the classical pseudo second order velocity equation is:

$$\frac{dq_t}{dt} = k_2(q_e - q_t)^2 \tag{14}$$

or

$$\frac{1}{q_t} = \frac{1}{k_2 q_e^2} + \frac{1}{q_e} t \tag{15}$$

transforming which you obtain:

$$q_t = \frac{t}{\frac{1}{k_2 q_e^2} + \frac{t}{q_e}}, \tag{16}$$

where k_2 — the adsorption rate constant of the pseudo second order model (g/mmol·min).

Linear plots of $\ln(q_e - q_t)$ versus t for a pseudo-first-order reaction and t/q_t versus t for a pseudo second order reaction for dye adsorption were tested to obtain rate parameters. Kinetic parameters under various conditions were calculated from these graphs. They are given in Table 3. The applied pseudo-first-order equation satisfactorily describes the regularities of adsorption at the initial stages (up to 60 min in the experiment) of the adsorption process, when the phenomenon of film diffusion has a significant effect on the process. An increase in the concentration of sorbate molecules at the adsorbent surface at the initial moments at low degrees of filling of the adsorption space stimulates the movement of sorbate molecules into the adsorbent pores under the influence of the concentration gradient, but subsequently this process slows down, which in turn potentiates other mechanisms. The calculated values of the determination coefficient make it possible to judge that the pseudo-first-order kinetic model of adsorption describes the process less accurately, and, therefore, the pseudo-second-order kinetic model is preferable.

Table 3

Kinetic parameters of the adsorption process

Adsorbent	t, °C	C_e, mg/g	Time to reach equilibrium, min	R^2		k_1, min^{-1}	k_2, g/mg min
				Pseudo first order	Pseudo second order		
Congo Red							
Nickel(II) trimesinate	10	31.2	165	0.898	0.946	$8\cdot10^{-3}$	$3.44\cdot10^{-3}$
	20	34.4	120	0.949	0.925	$6\cdot10^{-2}$	$0.2\cdot10^{-3}$
	35	35.2	105	0.943	0.984	$8.6\cdot10^{-2}$	$0.06\cdot10^{-3}$
Cobalt(II) trimesinate	10	34.3	60	0.989	0.948	$1.6\cdot10^{-2}$	$0.69\cdot10^{-3}$
	20	36.8	60	0.981	0.909	$1.1\cdot10^{-2}$	$0.32\cdot10^{-3}$
	35	37.2	45	0.979	0.954	$1\cdot10^{-2}$	$0.016\cdot10^{-3}$
Methylene blue							
Nickel(II) trimesinate	10	32.4	195	0.978	0.985	$6.8\cdot10^{-3}$	$3.2\cdot10^{-3}$
	20	32.8	180	0.999	0.996	$7.3\cdot10^{-3}$	$0.44\cdot10^{-3}$
	35	35	120	0.961	0.992	$9.2\cdot10^{-2}$	$0.073\cdot10^{-3}$
Cobalt(II) trimesinate	10	7	90	0.949	0.999	$6.9\cdot10^{-2}$	$0.25\cdot10^{-2}$
	20	9.4	75	0.991	0.988	0.137	$0.09\cdot10^{-2}$
	35	12.6	60	0.998	0.986	0.152	$0.04\cdot10^{-2}$

The activation energies of the adsorption process of dyes on nickel(II) and cobalt(II) trimesinates were calculated from the dependence of $\ln k_2$ on the reciprocal temperature (Fig. 5), which amounted to 5.15 (nickel(II) trimesinate – Congo Red), 2.99 (nickel(II) trimesinate – Methylene blue), 3.32 (cobalt(II) trimesinate – Congo Red), 1.44 kJ/mol (cobalt trimesinate – Methylene blue). The activation energies are small values, which indicates the feasibility of the adsorption process under these conditions, in addition, since all values are below 40 kJ/mol, it can be assumed with a reasonable degree of confidence that the limiting process is physical adsorption.

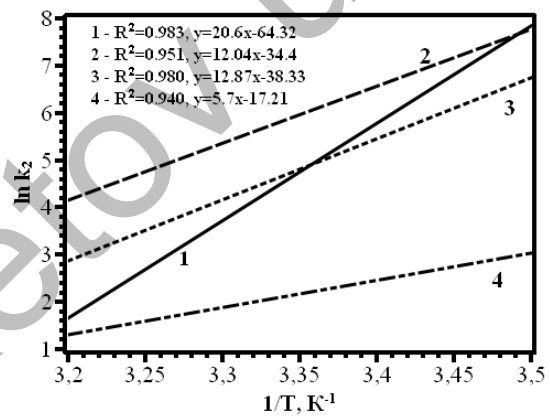

1 — Nickel(II) trimesinate – Congo Red; *2* — nickel(II) trimesinate – Methylene blue, *3* — cobalt(II) trimesinate – Congo Red; 4 — cobalt(II) trimesinate – Methylene blue

Figure 5. Dependence of the pseudo-second order adsorption rate constant on the reciprocal temperature for the systems

To determine the spontaneity of the adsorption process and verify the obtained experimental data, three main thermodynamic parameters were used, namely the change in enthalpy (ΔH_0), entropy (ΔS_0), and Gibbs free energy (ΔG_0). The Gibbs equation was used to study the effect of temperature on the equilibrium adsorption:

$$\Delta G^0 = -RT \ln K_c, \tag{17}$$

where K_c — the thermodynamic equilibrium constant, which can be determined from the equation

$$K_c = \frac{C_t}{C_e}. \tag{18}$$

Considering the change in concentrations in the real time interval and depending on the dose of the adsorbent, equation (19) can be written as:

$$K_c = \frac{(C_0 - C_e)V}{mC_e}. \quad (19)$$

The Gibbs equation can also be expressed as follows:

$$\Delta G^0 = \Delta H^0 - T\Delta S^0. \quad (20)$$

Combining the above equations, we obtain

$$lnK_c = \frac{\Delta S^0}{R} - \frac{\Delta H^0}{RT}. \quad (21)$$

The thermodynamic parameters of the process calculated graphically from the dependence of the thermodynamic equilibrium constant on the reciprocal temperature are given in Table 4.

Table 4

Thermodynamic parameters of the dye adsorption in the temperature range of 283–308 K

Adsorbent	Sorbate	T, K	K_c	ΔG^0, kJ/mol	ΔH^0, kJ/mol	ΔS^0, J/mol K
Nickel(II) trimesinate	Congo Red	283	7.1	–4.6	3.2	27.5
		293	12.3	–6.1		
		308	13.4	–6.6		
Nickel(II) trimesinate	Methylene blue	283	8.5	–5.03	3	28.3
		293	9.1	–5.35		
		308	14.6	–9.91		
Cobalt(II) trimesinate	Congo Red	283	11.3	–5.7	1.3	24.7
		293	23	–7.6		
		308	26.6	–8.44		
Cobalt(II) trimesinate	Methylene blue	283	0.42	–2.04	0.4	6.1
		293	0.61	–1.21		
		308	0.92	–0.23		

It can be seen from Table 4 that for the compounds under study, the adsorption process is characterized by negative values of the Gibbs free energy, and the enthalpy of the process takes positive values, which describes the process as a whole as endothermic. However, the adsorption of Methylene blue with cobalt(II) trimesinate has much lower Gibbs free energy and minimal enthalpy values compared to other systems, which can be explained by the competition of sorbate and water molecules on the sorbent surface. The decrease in the value of the Gibbs free energy with increasing temperature indicates a greater efficiency of adsorption at moderately elevated temperatures. The endothermic nature of adsorption under these conditions is explained by the need for the particles of the organic dye to reach the active centers of the adsorbent, and for this, they should be free from the hydration shell, or at least part of it, for which energy must be expended. As a result, the calculated value of enthalpy is the resultant of two processes, namely dehydration of organic dye ions (endothermic process) and adsorption of the latter on the active centers of the adsorbent, which proceeds with the release of energy (heat of adsorption). A positive entropy value indicates an increase in the number of degrees of freedom at the solid-liquid interface during the dye adsorption process and reflects the sorbate affinity for adsorbent molecules. An exception is the system cobalt trimesinate – Methylene blue, which is characterized by the low heat of adsorption and the loss of some degrees of freedom of the adsorbent in relation to Methylene blue in the adsorption process, which is confirmed by the low system entropy.

Conclusions

In this work, we developed an easily accessible procedure for the synthesis of nickel and cobalt trimesates in water in the presence of alkali. The possibility of using nickel and cobalt trimesinates for the adsorption of organic dyes from aqueous solutions was studied. Equilibrium adsorption data were analyzed using three typical adsorption models, namely Langmuir, Freundlich, and Temkin in the temperature range of 283–308 K. It was found that the adsorption of organic dyes on nickel and cobalt trimesinates was best described by the Freundlich isotherm equation. The values of thermodynamic parameters (ΔG^0, ΔH^0, ΔS^0) indicate the competitive advantage of sorbate molecules over solvent molecules in the case of adsorption of Congo Red by cobalt(II) and nickel(II) trimesinates, and in the case of methylene blue adsorption, water

molecules have a competitive advantage over sorbate molecules. Cobalt(II) trimesinate has a good ability to adsorb anionic dyes, while it shows an average adsorption activity for cationic dyes and can be used as a selective adsorbent.

Acknowledgments

This research was carried out in accordance with the state task, state registration number AAAA-A19-119041090087-4.

References

1 Dybtsev D.N. Homochiral metal–organic material with permanent porosity, enantioselective sorption properties, and catalytic activity / D.N. Dybtsev, A.L. Nuzhdin, H. Chun, K.P. Bryliakov, E.P. Talsi, V.P. Fedin, K.A. Kim // Angew. Chem. Int. Ed. — 2006. –Vol. 45, No. 6. — P. 916–920. https://doi.org/10.1002/anie.200503023

2 Dybtsev D.N. Microporous manganese formate: a simple metal−organic porous material with high framework stability and highly selective gas sorption properties / D.N. Dybtsev, H. Chun, S.H. Yoon, D. Kim, K. Kim // J. Am. Chem. Soc. — 2004. — Vol. 126, No. 1. — P. 32–33. https://doi.org/10.1021/ja038678c

3 Lin W. Supramolecular engineering of chiral and acentric 2D networks. synthesis, structures, and second-order nonlinear optical properties of bis(nicotinato)zinc and bis{3-[2-(4-pyridyl)ethenyl]benzoato}cadmium / W. Lin, O.R. Evans, R.-G. Xiong, Z. Wang // J. Am. Chem. Soc. — 1998. — Vol. 120, No. 50. — P. 13272–13273. https://doi.org/10.1021/ja983415h

4 Toma L.M. $[Mn_2(bipym)(H_2O)_8]^{4+}$ and $[Fe(bipy)(CN)_4]^-$ as building blocks in designing novel bipym- and cyanide-bridged heterobimetallic complexes (bipym = 2,2′-bipyrimidine and bipy = 2,2′-bipyridine) / L.M. Toma, R. Lescouzec, L.D. Toma, F. Lloret, M. Julve, J. Vaissermann, M. Andruh // J. Chem. Soc. Dalton Trans. — 2002. — No. 50. — P. 3171–3176. https://doi.org/10.1039/B202422P

5 Kitagawa S. Functional porous coordination polymers / S. Kitagawa, R. Kitaura, S.-i. Noro // Angew. Chem. Int. Ed. — 2004. — Vol. 43, No. 18. — P. 2334–2375. https://doi.org/10.1002/anie.200300610

6 Chui S.S.-Y. A Chemically functionalizable nanoporous material $[Cu_3(TMA)_2(H_2O)_3]_n$ / S.S.-Y. Chui, S.M.-F. Lo, J.P. Charmant, A.G. Orpen, I.D. Williams // Science. — 1999. — Vol. 283, No. 5405. — P. 1148–1150. https://doi.org/10.1126/science.283.5405.1148

7 Feldblyum J. I., Liu M., Gidley D. W., Matzger A. J. Reconciling the discrepancies between crystallographic porosity and guest access as exemplified by Zn-HKUST-1 // J. Am. Chem. Soc. — 2011. — Vol. 133, No. 45. — P. 18257–18263. https://doi.org/10.1021/ja2055935

8 Kramer M. Synthesis and properties of the metal-organic framework $Mo_3(BTC)_2$(TUDMOF-1) / M. Kramer, U. Schwarz, S. Kaskel // J. Mater. Chem. — 2006. — Vol. 16, No. 23. — P. 2245–2248. https://doi.org/10.1039/B601811D

9 Murray L.J. Highly-selective and reversible O_2 binding in Cr_3(1,3,5-benzenetricarboxylate)$_2$ / L.J. Murray, M. Dinca, J. Yano, S. Chavan, S. Bordiga, C.M. Brown, J.R. Long // J. Am. Chem. Soc. — 2010. — Vol. 132, No. 23. — P. 7856–7857. https://doi.org/10.1021/ja1027925

10 Sumida K., Her J.-H. J.-H., Dincă M., Murray L. J., Schloss J. M., Pierce C. J., Thompson B. A., FitzGerald S. A., Brown C. M., Long J. R. Neutron scattering and spectroscopic studies of hydrogen adsorption in $Cr_3(BTC)_2$ — A metal−organic framework with exposed Cr^{2+} sites // J. Phys. Chem. C. — 2011. — Vol. 115, No. 16. — P. 8414–8421. https://doi.org/10.1021/jp200638n.

11 Xie L. Mixed-valence iron(II, III) trimesates with open frameworks modulated by solvents / L. Xie, S. Liu, C. Gao, R. Cao, J. Cao, C. Sun, Z. Su // Inorg. Chem. – 2007. – Vol. 46, No. 19. — P. 7782–7788. https://doi.org/10.1021/ic062273m.

12 Maniam P. Investigation of porous Ni-based metal-organic frameworks containing paddle-wheel type inorganic building units via high-throughput methods / P. Maniam, N. Stock // Inorg. Chem. – 2011. – Vol. 50, No. 11. — P. 5085–5097. https://doi.org/10.1021/ic200381f.

13 Noei H. CO adsorption on a mixed-valence ruthenium metal-organic framework studied by UHV-FTIR spectroscopy and DFT calculations / H. Noei, O. Kozachuk, S. Amirjalayer, S. Bureekaew, M. Kauer, R. Schmid, B. Marler, M. Muhler, R.A. Fischer, Y. Wang // J. Phys. Chem. C. — 2013. — Vol. 117, No. 11. — P. 5658–5666. https://doi.org/10.1021/jp3056366.

14 Wade C.R. Investigation of the synthesis, activation, and isosteric heats of CO2 adsorption of the isostructural series of metal-organic frameworks $M_3(BTC)_2$ (M = Cr, Fe, Ni, Cu, Mo, Ru) / C.R. Wade, M. Dinca // Dalton Trans. — 2012. — Vol. 41, No. 26. — P. 7931–7938. https://doi.org/10.1039/C2DT30372H.

15 Marri S.R. Two novel 3D-MOFs (Ca-TATB and Co-HKUST): synthesis, structure and characterization / S.R. Marri, N. Chauhan, R.K. Tiwari, J. Kumar, J.N. Behera // Inorg. Chim. Acta. — 2018. — No. 478. — P. 8–14. https://doi.org/10.1016/j.ica.2018.03.014.

16 Suh M.P. Syntheses and functions of porous metallosupramolecular networks / M.P. Suh // Coord. Chem. Rev. — 2008. — Vol. 252. — P. 1007–1026. https://doi.org/10.1016/j.ccr.2008.01.032.

17 Dzhardimalieva G.I. Design and synthesis of coordination polymers with chelated units and their application in nanomaterials science / G.I. Dzhardimalieva, I.E. Uflyand // RSC Adv. — 2017. — Vol. 7, No. 67. — P. 42242–42288. https://doi.org/10.1039/C7RA05302A.

18 Dzhardimalieva G. I., Uflyand I.E. Chemistry of polymeric metal chelates / G.I. Dzhardimalieva, I.E. Uflyand. — Cham: Springer. — 2018. — P. 633–759.

19 Zhang H. Wire spherical-shaped Co-MOF electrode materials for high-performance all-solid-state flexible asymmetric supercapacitor device / H. Zhang, J. Wang, Y. Sun, X. Zhang, H. Yang, B. Lin // J. Alloys Compd. — 2021. — No. 879. — ID 160423. https://doi.org/10.1016/j.jallcom.2021.160423

20 Ramachandran R. Morphology-dependent electrochemical properties of cobalt-based metal organic frameworks for supercapacitor electrode materials / R. Ramachandran, C. Zhao, D. Luo, K. Wang, F. Wang // Electrochim. Acta. — 2018. — Vol. 267. — P. 170–180. https://doi.org/10.1016/j.electacta.2018.02.074

21 Horcajada P. Metal-Organic Frameworks in Biomedicine / P. Horcajada, R. Gref, T. Baati, P.K. Allan, G. Maurin, P. Couvreur, G. Ferey, R.E. Morris, C. Serre // Chem. Rev. — 2012. — Vol. 112. — P. 1232–1268. https://dx.doi.org/10.1021/cr200256v

22 Uflyand I.E. Recent strategies to improve MOF performance in solid phase extraction of organic dyes / I.E. Uflyand, V.A. Zhinzhilo, V.O. Nikolaevskaya, B.I. Kharisov, C.M. Oliva González, O.V. Kharissova // Microchem. J. — 2021. — No. 168. — ID 106387. https://doi.org/10.1016/j.microc.2021.106387

23 Yu G. Cobalt-based metal organic framework as precursor to achieve superior catalytic activity for aerobic epoxidation of styrene / G. Yu, J. Sun, F. Muhammad, P. Wang, G. Zhu // RSC Adv. — 2014. — Vol. 4, No. 73. — P. 38804–38811. https://doi.org/10.1039/C4RA03746D

24 Zhu H.-F. Hydrothermal synthesis and structural characterization of one-dimensional coordination polymers of cobalt(II) and nickel(II) with 1,3,5-benzenetriacetic acid / H.-F. Zhu, W.-Y. Sun, T. Okamura, N. Ueyama // Inorg. Chem. Commun. — 2003. — Vol. 6, No. 2. — P. 168–173. https://doi.org/10.1016/S1387-7003(02)00714-1

25 Дыбцев Д.Н. Синтез, структура и магнитные свойства слоистого координационного полимера 1,3,5-бензолтрикарбоксилата кобальта (II) / Д.Н. Дыбцев, М.П. Юткин, Е.В. Пересыпкина, А.В. Вировец, Й. Хасегава, Х. Ниши-хара, В.П. Федин // Изв. РАН. Сер. хим. — 2007. — № 9. — С. 1719–1723. https://doi.org/10.1007/s11172-007-0277-8

26 Lu H.-S. Surfactant media to grow new crystalline cobalt 1,3,5-benzenetricarboxylate metal−organic frameworks / H.-S. Lu, L. Bai, W.-W. Xiong, P. Li, J. Ding, G. Zhang, T. Wu, Y. Zhao, J.-M. Lee, Y. Yang, B. Geng, Q. Zhang // Inorg. Chem. — 2014. — Vol. 53, No. 16. — P. 8529−8537. https://doi.org/10.1021/ic5011133

27 Neff H. Periodic protein adsorption at the gold/biotin aqueous solution interface: evidence of kinetics with time delay / H. Neff, H.M. Laborde, A.M.N. Lima // Sci. Rep. — 2016. — Vol. 6. — ID 36232. https://doi.org/10.1038/srep36232

28 Dzhardimalieva G. Synthesis of copper(II) trimesinate coordination polymer and its use as a sorbent for organic dyes and a precursor for nanostructured material / G. Dzhardimalieva, R. Baimuratova, E. Knerelman, G. Davydova, S. Kudaibergenov, O. Kharissova, V. Zhinzhilo, I. Uflyand // Polymers. — 2020. — Vol. 12, No. 5. — ID 1024. https://doi.org/10.3390/polym12051024

29 Yaghi O. M. Construction of porous solids from hydrogen-bonded metal complexes of 1,3,5-benzenetricarboxylic acid / O.M. Yaghi, H. Li, T.L. Groy // J. Am. Chem. Soc. — 1996. — Vol. 118, No. 38. — P. 9096–9101. https://doi.org/10.1021/ja960746q

30 Wang S. A comparative study of dye removal using fly ash treated by different methods / S. Wang, Y. Boyjoo, A. Choueib // Chemosphere. — 2005. — Vol. 60, No. 10. — P. 1401–1407. https://doi.org/10.1016/j.chemosphere.2005.01.091

31 Hameed B.H. A novel agricultural waste adsorbent for the removal of cationic dye from aqueous solutions / B.H. Hameed, R.R. Krishni, S.A. Sata // J. Hazard. Mater. — 2009. — Vol. 162, No. 1. — P. 305–311. https://doi.org/10.1016/j.jhazmat.2008.05.036

32 Hamdaoui O. Batch study of liquid-phase adsorption of methylene blue using cedar sawdust and crushed brick / O. Hamdaoui // J. Hazard. Mater. — 2006. — No. 135. — P. 264–273. https://doi.org/10.1016/j.jhazmat.2005.11.062.

33 Halsey G.D. The role of surface heterogeneity in adsorption / G.D. Halsey // Adv. Catal. — 1952. — Vol. 4. — P. 259–269. https://doi.org/10.1016/S0360-0564(08)60616-1

34 Dada A.O. Langmuir, Freundlich, Temkin and Dubinin-Radushkevich isotherms studies of equilibrium sorption of Zn^{2+} unto phosphoric acid modified rice husk / A.O. Dada, A.P. Olalekan, A.M. Olatunya, O. Dada // IOSR J. Appl. Chem. — 2012. — Vol. 3, No. 1. — P. 38–45. https://doi.org/10.9790/5736-0313845

35 Simonin J.-P. On the comparison of pseudo-first order and pseudo-second order rate laws in the modeling of adsorption kinetics / J.-P. Simonin // Chem. Eng. J. — 2016. — No. 300. — P. 254–263. https://doi.org/10.1016/j.cej.2016.04.079

В.А. Жинжило, А.Ю. Литвинова, В.М. Лямина, Г.И. Джардималиева, И.Е. Уфлянд

Органикалық бояғыштардың перспективті адсорбенттері ретінде никель және кобальт тримезинаттар негізіндегі координациялық полимерлер

Металлорганикалық каркастары (МОК) көпіршікті органикалық лигандтарды байланыстыратын металл иондарынан тұратын кристалдық қосылыстар. Металдың координациялық геометриясынан және донор атомдарының байланыс бағытына, сондай-ақ көпіршікті лигандтың геометриясына байланысты 1D, 2D, немесе 3D полимер құрылымдары түзіледі. Металлорганикалық каркастардың сипатты белгілері төмен тығыздық, жоғары кеуектілік пен кристалдылық және үлкен меншікті бетінің

ауданы болып табылады. Мұндай материалдарды жасаудың технологиялық аспектілеріне және оларды әртүрлі құрылғыларға біріктіруге көп көңіл бөлінеді. МОК алу үшін гидротермиялық және солвотермиялық синтезді қоса алғанда, бөлме температурасында және конвективтік қыздыру кезінде тұндыру реакцияларына негізделген әртүрлі синтетикалық тәсілдер әзірленген. Бұл жұмыста никель ацетаты мен кобальт нитратына сілтінің қатысуымен тримезин қышқылымен әрекеттесуі арқылы модификацияланған әдіспен никель және кобальт тримезинаттары негізіндегі металлорганикалық каркастық құрылымдар синтезделді. Алынған қосылыстар конго қызылы және метилен көгі органикалық бояғыштарының сулы ерітінділерінен адсорбциялануын зерттеу үшін пайдаланылды. Адсорбция дәрежесі температураға байланысты және шамасы конго қызылы үшін 97 % дейін жетеді, сол уақытта шама метилен көгі үшін 83 % құрайды. Адсорбция процесінің механизмдері мен сипаттамалық параметрлері Лангмюр, Темкин және Фрейндлих изотермаларының эмпирикалық үлгілері арқылы талданған, олардың ішінде адсорбция процесі Фрейндлих моделімен оптималды түрде сипатталған. Есептелген термодинамикалық параметрлер процестің өздігінен жүретіндігін және оның елеусіз эндотермиялық сипатын көрсетеді.

Кілт сөздер: металлорганикалық каркас құрылымдары, координациялық полимерлер, тримез қышқылы, ластаушы заттар, адсорбция, конго қызылы, метилен көгі, термодинамикалық параметрлер, адсорбция изотермалары, адсорбциялық сыйымдылық.

В.А. Жинжило, А.Ю. Литвинова, В.М. Лямина, Г.И. Джардималиева, И.Е. Уфлянд

Координационные полимеры на основе тримезинатов никеля и кобальта как перспективные адсорбенты органических красителей

Металлоорганические каркасы (МОК) представляют собой кристаллические соединения, состоящие из ионов металлов, координированных мостиковыми органическими лигандами. В зависимости от координационной геометрии металла и направления связи донорных атомов, а также от геометрии мостикового лиганда формируются 1D-, 2D- или 3D-структуры полимера. Характерными особенностями металлоорганических каркасов являются низкая плотность, высокая пористость и кристалличность, большая удельная поверхность. Особое внимание уделено технологическим аспектам создания таких материалов и их интеграции в различные устройства. Для получения МОК разработаны различные синтетические подходы, основанные на реакциях осаждения при комнатной температуре и при конвективном нагреве, включая гидротермальный и сольвотермальный синтез. В настоящей статье металлоорганические каркасные структуры на основе тримезинатов никеля и кобальта были синтезированы по модифицированной методике взаимодействием ацетата никеля и нитрата кобальта с тримезиновой кислотой в присутствии щелочи. Полученные соединения использованы для изучения адсорбции органических красителей конго красного и метиленового синего из их водных растворов. Степень адсорбции зависит от температуры и достигает величины 97 % для конго красного, в то время как для метиленового синего она составляет порядка 83 %. Механизмы и характерные параметры процесса адсорбции проанализированы с применением эмпирических моделей изотерм Ленгмюра, Темкина и Фрейндлиха, из которых оптимально процесс адсорбции описывается моделью Фрейндлиха. Рассчитанные термодинамические параметры указывают на самопроизвольность процесса и незначительный его эндотермический характер.

Ключевые слова: металлоорганические каркасные структуры, координационные полимеры, тримезиновая кислота, поллютанты, адсорбция, конго красный, метиленовый синий, термодинамические параметры, изотермы адсорбции, адсорбционная емкость.

References

1 Dybtsev, D.N., Nuzhdin, A.L., Chun, H., Bryliakov, K.P., Talsi, E.P., Fedin, V.P., & Kim, K.A. (2006). Homochiral metal–organic material with permanent porosity, enantioselective sorption properties, and catalytic activity. *Angew. Chem. Int. Ed., 45* (6), 916–920. https://doi.org/10.1002/anie.200503023

2 Dybtsev, D.N., Chun, H., Yoon, S.H., Kim, D., & Kim, K. (2004). Microporous manganese formate: a simple metal−organic porous material with high framework stability and highly selective gas sorption properties. *J. Am. Chem. Soc., 126* (1), 32–33. https://doi.org/10.1021/ja038678c.

3 Lin, W., Evans, O.R., Xiong, R.-G., & Wang, Z. (1998). Supramolecular engineering of chiral and acentric 2D networks. synthesis, structures, and second-order nonlinear optical properties of bis(nicotinato)zinc and bis{3-[2-(4-pyridyl)ethenyl]benzoato}cadmium. *J. Am. Chem. Soc. 120* (50), 13272–13273. https://doi.org/10.1021/ja983415h.

4 Toma, L.M., Lescouzec, R., Toma, L.D., Lloret, F., Julve, M., Vaissermann, J., & Andruh, M. (2002). $[Mn_2(bipym)(H_2O)_8]^{4+}$ and $[Fe(bipy)(CN)_4]^-$ as building blocks in designing novel bipym- and cyanide-bridged heterobimetallic complexes (bipym = 2,2′-bipyrimidine and bipy = 2,2′-bipyridine*). J. Chem. Soc. Dalton Trans.*, (50), 3171–3176. https://doi.org/10.1039/B202422P.

5 Kitagawa, S., Kitaura, R., & Noro, S.-I. (2004). Functional porous coordination polymers. *Angew. Chem. Int. Ed.*, *43* (18), 2334–2375. https://doi.org/10.1002/anie.200300610

6 Chui, S.S.-Y., Lo, S.M.-F., Charmant, J.P., Orpen, A.G., & Williams, I.D. (1999). A Chemically functionalizable nanoporous material $[Cu_3(TMA)_2(H_2O)_3]_n$. *Science, 283* (5405), 1148–1150. https://doi.org/10.1126/science.283.5405.1148

7 Feldblyum, J.I., Liu, M., Gidley, D.W., & Matzger A.J. (2011). Reconciling the discrepancies between crystallographic porosity and guest access as exemplified by Zn-HKUST-1. *J. Am. Chem. Soc.*, *133* (45), 18257–18263. https://doi.org/10.1021/ja2055935.

8 Kramer, M., Schwarz, U., & Kaskel, S. (2006). Synthesis and properties of the metal-organic framework $Mo_3(BTC)_2$(TUDMOF-1). *J. Mater. Chem.*, *16* (23), 2245–2248. https://doi.org/10.1039/B601811D.

9 Murray, L.J., Dinca, M., Yano, J., Chavan, S., Bordiga, S., Brown, C.M., & Long, J.R. (2010). Highly-selective and reversible O2 binding in Cr_3(1,3,5-benzenetricarboxylate)$_2$. *J. Am. Chem. Soc.*, *132* (23), 7856–7857. https://doi.org/10.1021/ja1027925.

10 Sumida, K., Her, J.-H., Dincă, M., Murray, L.J., Schloss, J.M., Pierce, C.J., Thompson, B.A., FitzGerald, S.A., Brown, C.M., & Long, J.R. (2011). Neutron scattering and spectroscopic studies of hydrogen adsorption in $Cr_3(BTC)_2$ — A metal−organic framework with exposed Cr^{2+} sites. *J. Phys. Chem. C.*, *115* (16), 8414–8421. https://doi.org/10.1021/jp200638n.

11 Xie, L., Liu, S., Gao, C., Cao, R., Cao, J., Sun, C., & Su, Z. (2007). Mixed-valence iron(II, III) trimesates with open frameworks modulated by solvents. *Inorg. Chem.*, *46* (19), 7782–7788. https://doi.org/10.1021/ic062273m.

12 Maniam, P., & Stock, N. (2011). Investigation of porous Ni-based metal-organic frameworks containing paddle-wheel type inorganic building units via high-throughput methods. *Inorg. Chem.*, *50* (11), 5085–5097. https://doi.org/10.1021/ic200381f.

13 Noei, H., Kozachuk, O., Amirjalayer, S., Bureekaew, S., Kauer, M., Schmid, R., Marler, B., Muhler, M., Fischer, R.A., & Wang, Y. (2013). CO adsorption on a mixed-valence ruthenium metal-organic framework studied by UHV-FTIR spectroscopy and DFT calculations. *J. Phys. Chem. C.*, *117* (11), 5658–5666. https://doi.org/10.1021/jp3056366.

14 Wade, C.R., & Dinca, M. (2012). Investigation of the synthesis, activation, and isosteric heats of CO_2 adsorption of the isostructural series of metal-organic frameworks $M_3(BTC)_2$ (M = Cr, Fe, Ni, Cu, Mo, Ru). *Dalton Trans.*, *41* (26), 7931–7938. https://doi.org/10.1039/C2DT30372H.

15 Marri, S.R., Chauhan, N., Tiwari, R.K., Kumar, J., & Behera, J.N. (2018). Two novel 3D-MOFs (Ca-TATB and Co-HKUST): synthesis, structure and characterization. *Inorg. Chim. Acta*, *478*, 8–14. https://doi.org/10.1016/j.ica.2018.03.014.

16 Suh, M.P. (2008). Syntheses and functions of porous metallosupramolecular networks. *Coord. Chem. Rev.*, *252*, 1007–1026. https://doi.org/10.1016/j.ccr.2008.01.032.

17 Dzhardimalieva, G.I., & Uflyand, I.E. (2017). Design and synthesis of coordination polymers with chelated units and their application in nanomaterials science. *RSC Adv.*, *7* (67), 42242–42288. https://doi.org/10.1039/C7RA05302A.

18 Dzhardimalieva, G.I., & Uflyand, I.E. (2018). Chemistry of polymeric metal chelates. Cham: Springer, 633–759.

19 Zhang, H., Wang, J., Sun, Y., Zhang, X., Yang, H., & Lin, B. (2021). Wire spherical-shaped Co-MOF electrode materials for high-performance all-solid-state flexible asymmetric supercapacitor device. *J. Alloys Compd.*, (879), 160423. https://doi.org/10.1016/j.jallcom.2021.160423.

20 Ramachandran, R., Zhao, C., Luo, D., Wang, K., & Wang, F. (2018). Morphology-dependent electrochemical properties of cobalt-based metal organic frameworks for supercapacitor electrode materials. *Electrochim. Acta*, *267*, 170–180. https://doi.org/10.1016/j.electacta.2018.02.074

21 Horcajada, P., Gref, R., Baati, T., Allan, P.K., Maurin, G., Couvreur, P., Ferey, G., Morris, R.E., & Serre C. (2012). Metal_Organic Frameworks in Biomedicine. Chem. Rev., 112, 1232–1268. https://dx.doi.org/10.1021/cr200256v

22 Uflyand, I.E., Zhinzhilo, V.A., Nikolaevskaya, V.O., Kharisov, B.I., Oliva, González, C.M., & Kharissova, O.V. (2021). Recent strategies to improve MOF performance in solid phase extraction of organic dyes. Microchem. J., (168), 106387. https://doi.org/10.1016/j.microc.2021.106387.

23 Yu, G., Sun, J., Muhammad, F., Wang, P., & Zhu, G. (2014). Cobalt-based metal organic framework as precursor to achieve superior catalytic activity for aerobic epoxidation of styrene. *RSC Adv.*, *4* (73), 38804–38811. https://doi.org/10.1039/C4RA03746D

24 Zhu, H.-F., Sun, W.-Y., Okamura, T., & Ueyama, N. (2003). Hydrothermal synthesis and structural characterization of one-dimensional coordination polymers of cobalt(II) and nickel(II) with 1,3,5-benzenetriacetic acid. *Inorg. Chem. Commun. 6* (2), 168–173. https://doi.org/10.1016/S1387-7003(02)00714-1

25 Dybtsev, D.N., Yutkin, M.P., Peresypkina, E.V., Virovets, A.V., Hasegawa, Y., Nishihara, H., & Fedin, V.P. (2007). Sintez, struktura i magnitnye svoistva sloistogo koordinatsionnogo polimera 1,3,5-benzoltrikarboksilata kobalta (II) [Synthesis, structure, and magnetic properties of the cobalt(II) 1,3,5-benzenetricarboxylate layered coordination polymer]. Izvestiia Rossiiskoi akademii nauk. Seriia khimicheskaia — *Bulletin of the Russian Academy of Sciences. Chemical series*, *56* (9), 1782–1786. https://doi.org/10.1007/s11172-007-0277-8 [in Russian].

26 Lu, H.-S., Bai, L., Xiong, W.-W., Li, P., Ding, J., Zhang, G., Wu, T., Zhao, Y., Lee, J.-M., Yang, Y., Geng, B., & Zhang, Q. (2014). Surfactant media to grow new crystalline cobalt 1,3,5-benzenetricarboxylate metal−organic frameworks. *Inorg. Chem.*, *53* (16), 8529−8537. https://doi.org/10.1021/ic5011133

27 Neff, H., Laborde, H.M., & Lima, A.M.N. (2016). Periodic protein adsorption at the gold/biotin aqueous solution interface: evidence of kinetics with time delay. *Sci. Rep.*, *6*, 36232. https://doi.org/10.1038/srep36232

28 Dzhardimalieva, G., Baimuratova, R., Knerelman, E., Davydova, G., Kudaibergenov, S., Kharissova, O., Zhinzhilo, V., & Uflyand, I. (2020). Synthesis of copper(II) trimesinate coordination polymer and its use as a sorbent for organic dyes and a precursor for nanostructured material. *Polymers*, *12* (5), 1024. https://doi.org/10.3390/polym12051024.

29 Yaghi, O.M., Li, H., & Groy, T.L. (1996). Construction of porous solids from hydrogen-bonded metal complexes of 1,3,5-benzenetricarboxylic acid. *J. Am. Chem. Soc., 118* (38), 9096–9101. https://doi.org/10.1021/ja960746q.

30 Wang, S., Boyjoo, Y., & Choueib, A. (2005). A comparative study of dye removal using fly ash treated by different methods. *Chemosphere, 60* (10), 1401–1407. https://doi.org/10.1016/j.chemosphere.2005.01.091.

31 Hameed, B.H., Krishni, R.R., & Sata, S.A. (2009). A novel agricultural waste adsorbent for the removal of cationic dye from aqueous solutions. *J. Hazard. Mater., 162* (1), 305–311. https://doi.org/10.1016/j.jhazmat.2008.05.036

32 Hamdaoui, O. (2006). Batch study of liquid-phase adsorption of methylene blue using cedar sawdust and crushed brick. *J. Hazard. Mater.*, (135), 264–273. https://doi.org/10.1016/j.jhazmat.2005.11.062

33 Halsey, G.D. (1952). The role of surface heterogeneity in adsorption. *Adv. Catal., 4*, 259–269. https://doi.org/10.1016/S0360-0564(08)60616-1.

34 Dada, A. O., Olalekan, A. P., Olatunya, A. M., & Dada, O. (2012). Langmuir, Freundlich, Temkin and Dubinin-Radushkevich isotherms studies of equilibrium sorption of Zn^{2+} unto phosphoric acid modified rice husk. *IOSR J. Appl. Chem., 3* (1), 38–45. https://doi.org/10.9790/5736-0313845

35 Simonin, J.-P. (2016). On the comparison of pseudo-first order and pseudo-second order rate laws in the modeling of adsorption kinetics. *Chem. Eng. J.*, (300), 254–263. https://doi.org/10.1016/j.cej.2016.04.079.

Information about authors*

Zhinzhilo, Vladimir Anatolievich — Candidate of Chemical Sciences, Senior Lecturer, Chemistry Department, Southern Federal University, Zorge Str. 7, Rostov-on-Don 344090, Russian Federation; e-mail i06993@yandex.ru; http://orcid.org/0000-0001-8423-7205;

Litvinova, Alena Yurievna — 5th year student, Chemistry Department, Southern Federal University, Zorge Str. 7, Rostov-on-Don 344090, Russian Federation; e-mail: chemist01@mail.ru; https://orcid.org/0000-0003-1416-4754;

Lyamina, Veronika Mikhailovna — 5th year student, Chemistry Department, Southern Federal University, Zorge Str. 7, Rostov-on-Don 344090, Russian Federation; e-mail: veronichka.lyamina@yandex.ru: https://orcid.org/0000-0001-5834-6600

Dzhardimalieva, Gulzhian Iskakovna (*corresponding author*) – Doctor of Chemical Sciences, Head of Laboratory of Metallopolymers, Institute of Problems of Chemical Physics Russian Academy of Sciences, Chernogolovka, Moscow Region, and Professor of Moscow Aviation Institute (National Research University), Moscow, Russia; e-mail: dzhardim@icp.ac.ru; https://orcid.org/0000-0002-4727-8910;

Uflyand, Igor Efimovich — Doctor of Chemical Sciences, Professor, Chemistry Department, Southern Federal University, Zorge Str. 7, Rostov-on-Don 344090, Russian Federation; e-mail: ieuflyand@sfedu.ru; http://orcid.org/0000-0002-7164-8168

*The author's name is presented in the order: *Last Name, First and Middle Names*